TERRADUE

Advancing Earth Science

Introduction to SAR Data Applications for Arctic Research

Pedro Gonçalves

Terradue

Research School on Cross-Disciplinary Science in the Arctic and Collaboration with Local Communities

02 – 07 December 2018 UNIS, Longyearbyen, Svalbard

The Research Council of Norway

INTAROS

Objectives

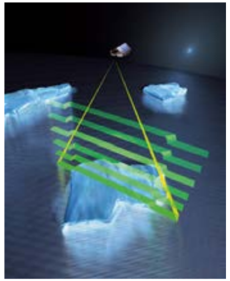

- Short review of existing radar sensors
- Introduce the different applications of SAR data to
  - map sea ice concentration
  - derive geophysical variables and products
  - focus over glaciers and ice sheets
- Followed by a hands-on exercise on those issues

SAREDU Remote Sensing Education Initiative

ellip Collaborative Earth Science Services

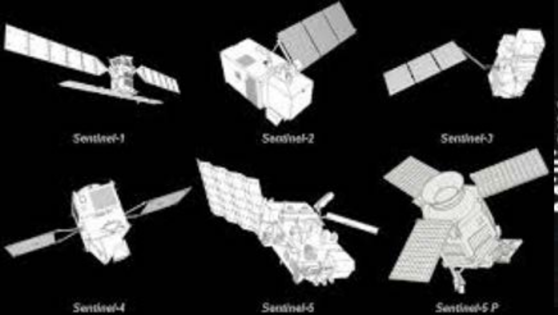

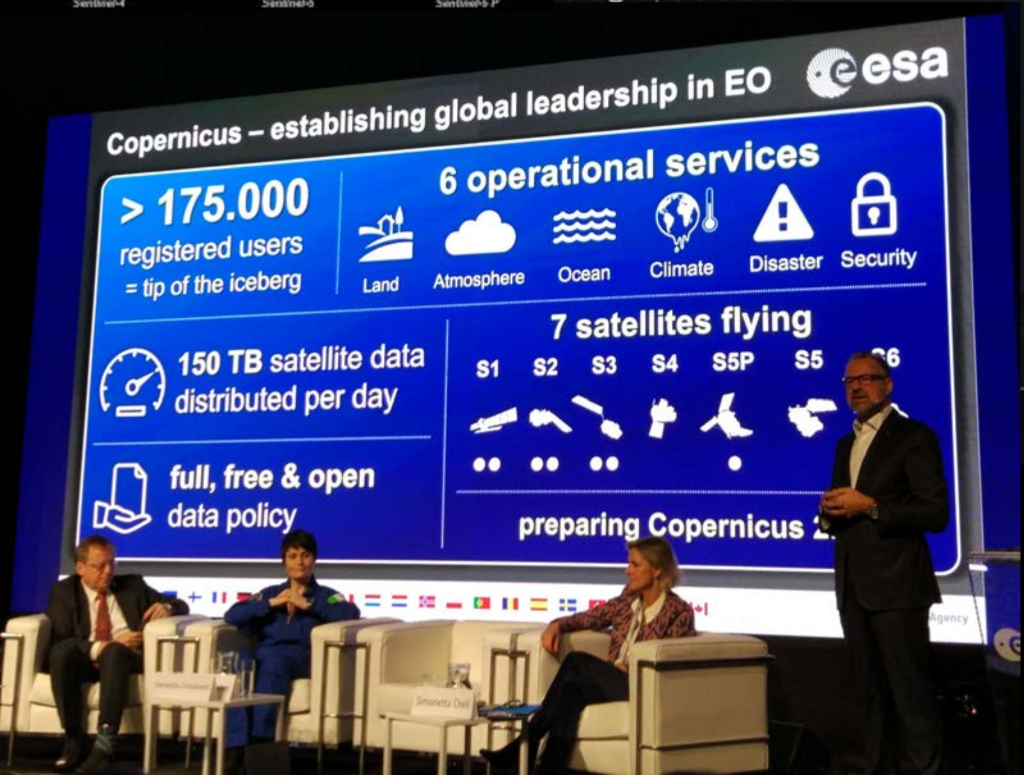

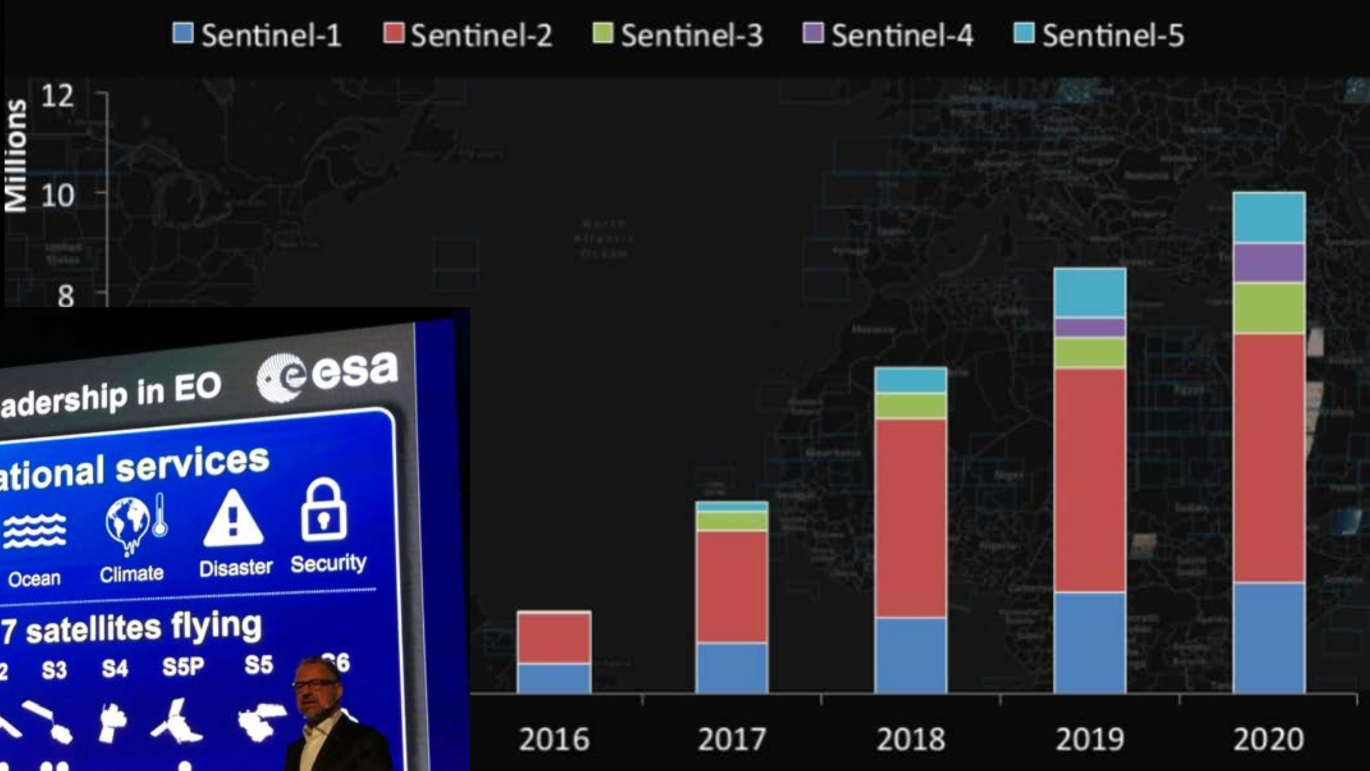

Copernicus Sentinels as the next generation Earth Observation satellites

Typical EO data volumes

500MB (S-2) < a single product < 8GB (S-1)

Radar Sensors

Four main types of spaceborne radar systems:

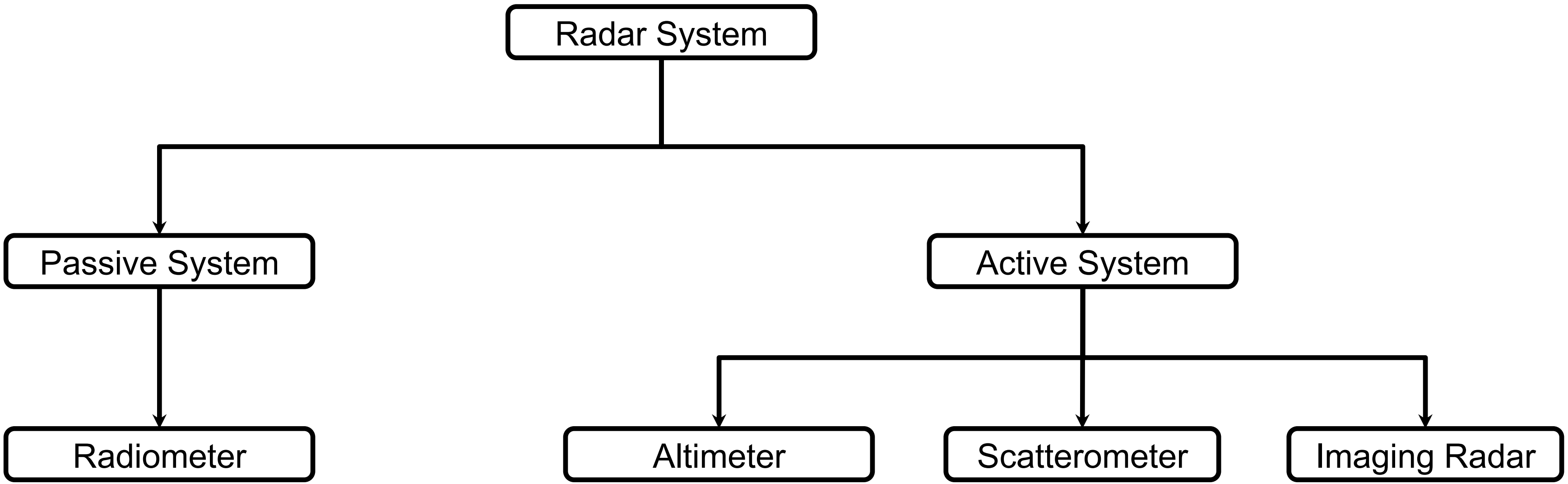

Radar Sensors

- Radiometers
  - Passive devices measuring the self-emission of the Earth's surface in the microwave region of electromagnetic spectrum
  - Measures spontaneous thermal radiations
  - Brightness depends on physical temperature and frequency

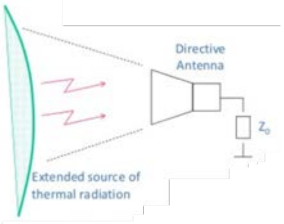

- Altimeters
  - Active devices measuring distances (calculated from signal travel time and speed of light)

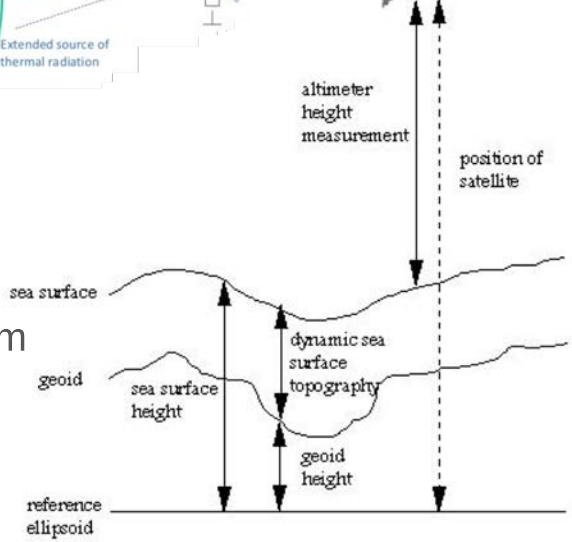

Radar Sensors

- Scatterometers
  - Active device measuring the energy scattered back from the surface with high radiometric resolution
  - It records the change in radar reflectivity of the sea due to the perturbation of small ripples by the wind close to the surface
  - Since the energy in these ripples increases with wind velocity, backscatter increases with wind velocity

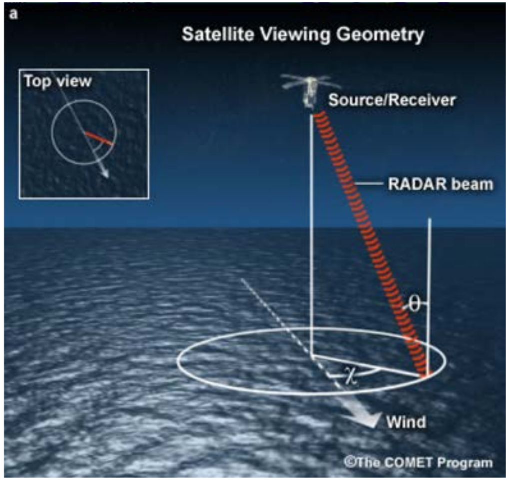

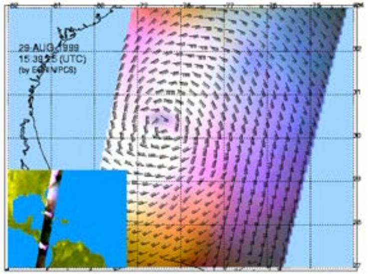

Radar Sensors

- SAR
  - Active device measuring the energy scattered back from the surface with high geometric resolution

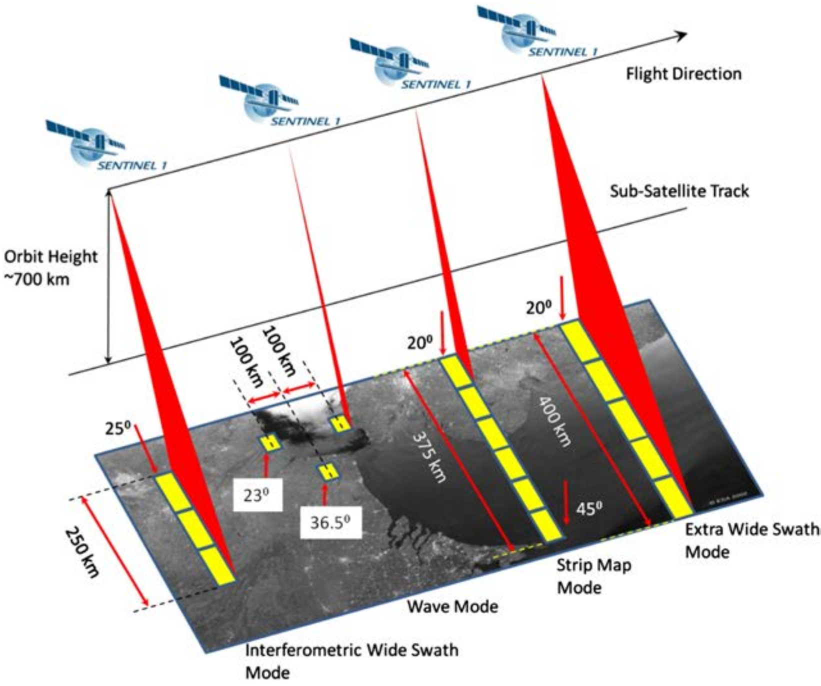

SAR Imaging Geometry

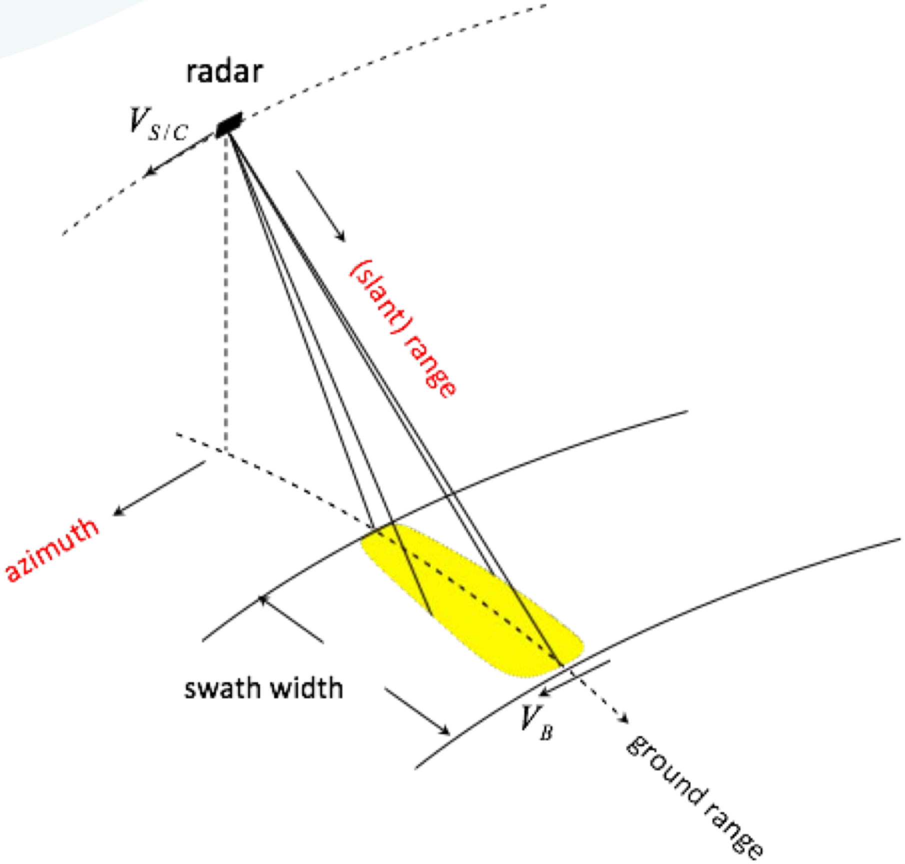

Radar transmits pulses and receives echoes at the rate of the pulse repetition frequency: *PRF* ≅ 1000 - 4000 Hz

range: radar principle = scanning at speed of light

azimuth: scanning in flight direction at V_B plus aperture synthesis (holography)

coherent imaging: complex-valued pixels contain amplitude (brightness) and phase information

for this lecture: straight flight path

$$\Rightarrow \quad V_{S/C} = V_B = V$$

Two-Step Imaging Process

- SAR is a two-step imaging process:

  1. Data acquisition
  Illumination of a scattering object and collection of received echoes ⇒ raw data
  Contribution of a single point is dispersed over $10^4 \ldots 10^7$ samples

  2. Processing
  Raw data focusing ⇒ image of the object

SAR Raw Data (After Range Compression)

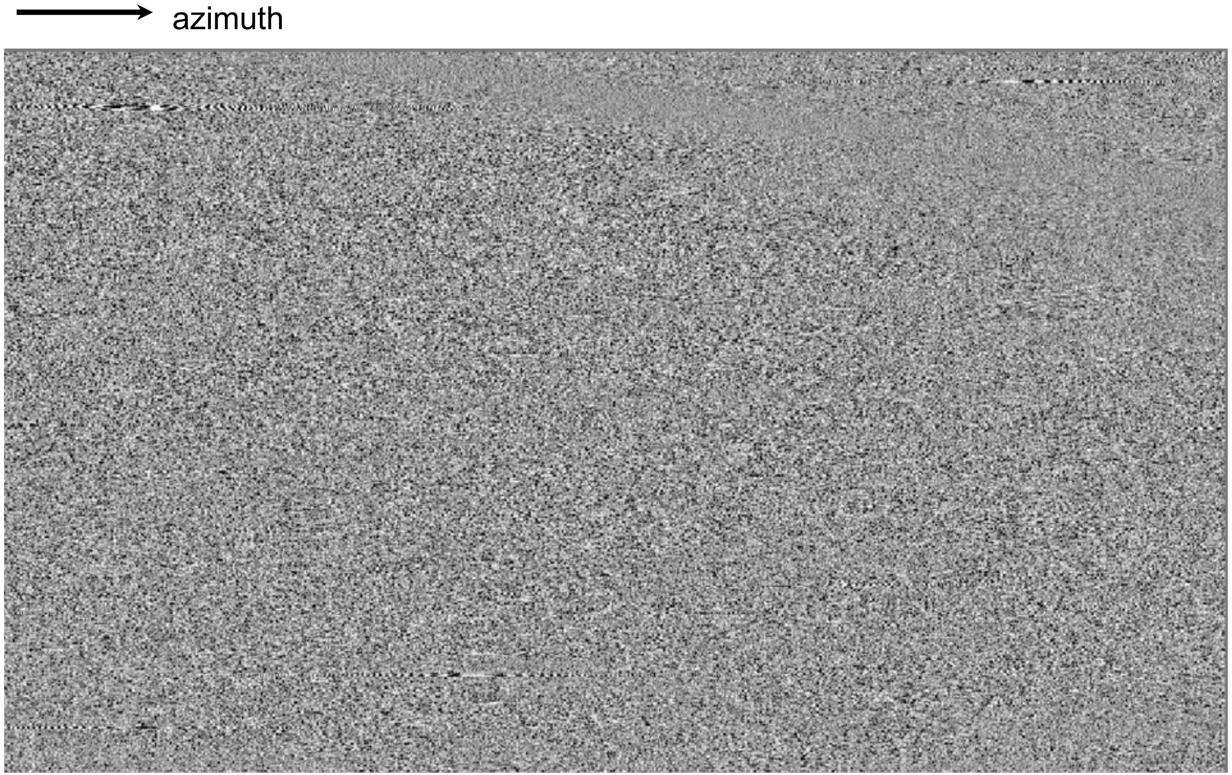

Focussed SAR Data

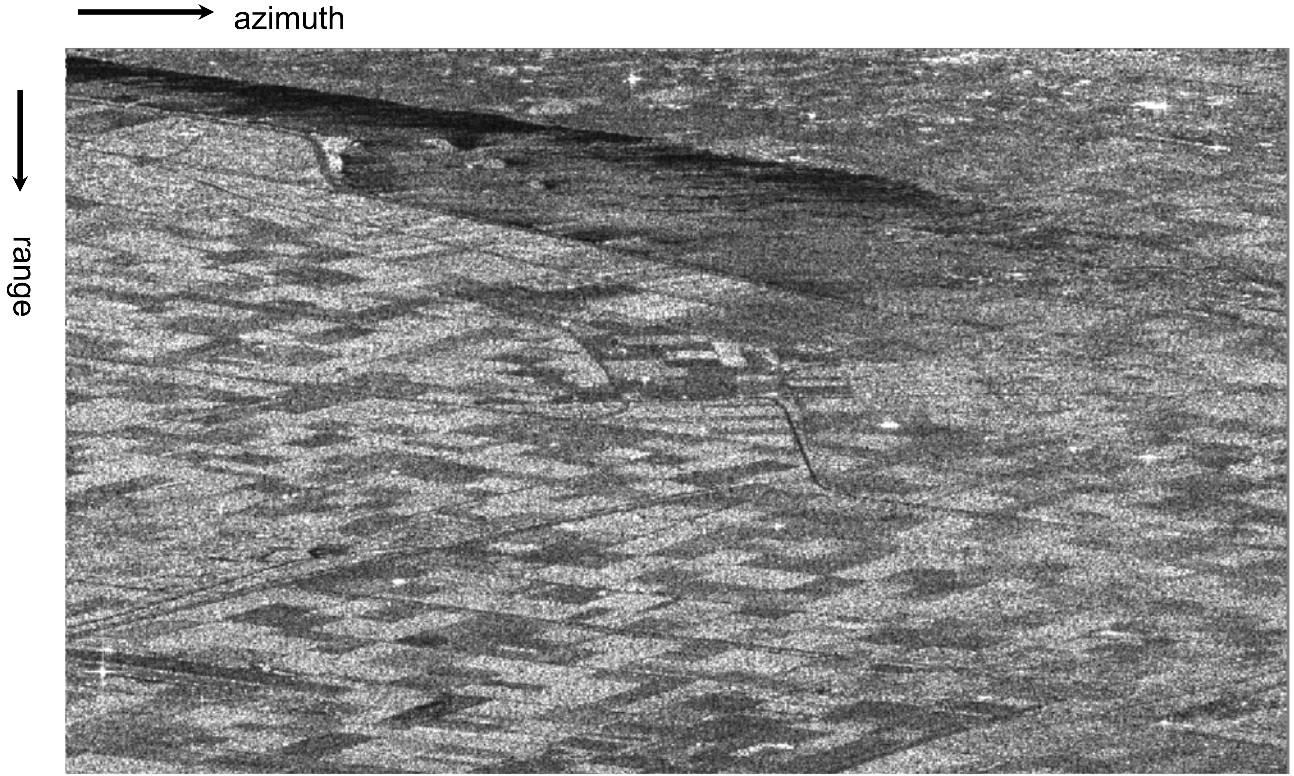

Focussed SAR Data

after
azimuth pixel averaging by 4
to achieve approximately
square pixels

Image Tone

- Refers to each distinguishable grey level from black to white
- Proportional to strength of radar backscatter
  - Relatively smooth targets like calm water appear as dark tones
  - Diffuse targets like some vegetation appear as intermediate tones
- Human-made targets (buildings, ships) may produce bright tones, depending on their shape, orientation and/or constituent materials

Parameters Influencing Radar Brightness

- Sensor Parameters
  - wavelength (e.g. penetration through canopy)
  - polarization, look angle and resolution (texture)
- Scene Parameters
  - surface roughness (e.g. Bragg scattering at ocean surfaces)
  - local slope and orientation ⇐ geomorphology
  - scatterer density, e.g. biomass, leaf density
  - 3-D distribution of scatterers and scattering mechanism, e.g. surface, volume, or double bounce (canopy, trunks, buildings)

Image Tone – Backscatter mechanisms

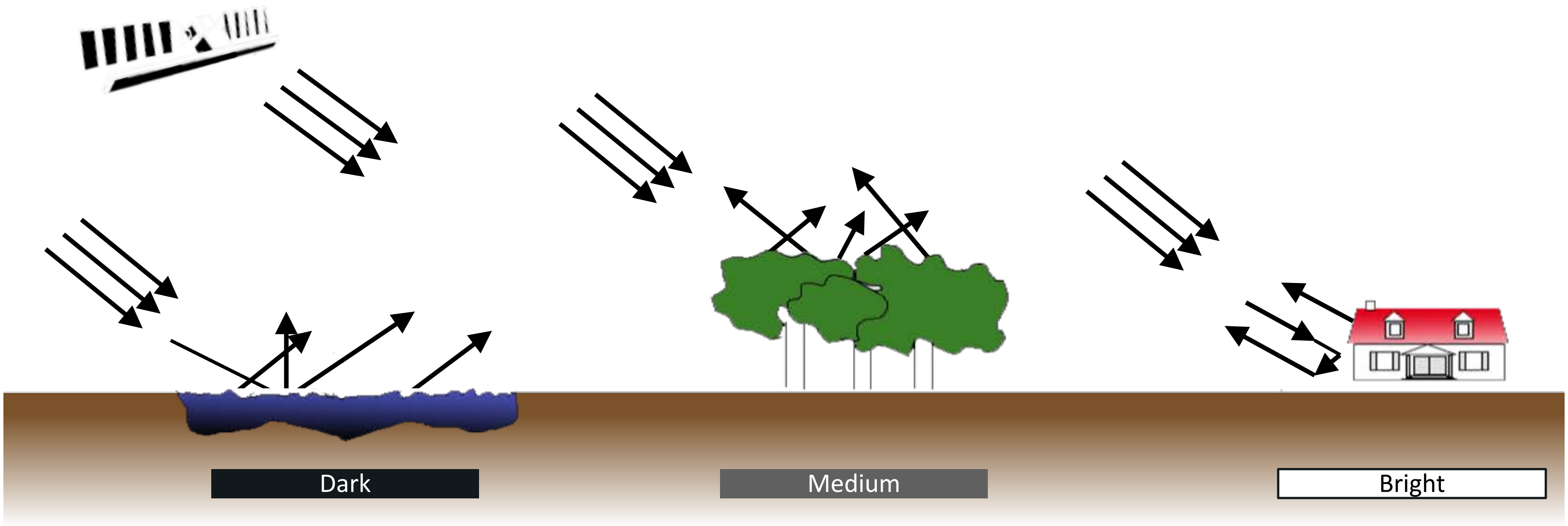

Microwave Frequency & Wavelength Bands

band	frequency	wavelength	typical application
	f_0	$\lambda = c / f_0$	
Ka	27 – 40 GHz	1.1 – 0.8 cm	airport surveillance
K	18 – 27 GHz	1.7 – 1.1 cm	little used (H_2O absorption)
Ku	12 – 18 GHz	2.4 – 1.7 cm	**satellite altimetry**
X	8 – 12 GHz	3.8 – 2.4 cm	**SAR**, marine radar, weather radar
C	4 – 8 GHz	7.5 – 3.8 cm	**SAR**, weather radar
S	2 – 4 GHz	15 – 7.5 cm	long-range weather radar
L	1 – 2 GHz	30 – 15 cm	**SAR**, traffic control
P	0.3 – 1 GHz	100 – 30 cm	experimental SAR

Scattering & Microwaves Penetration

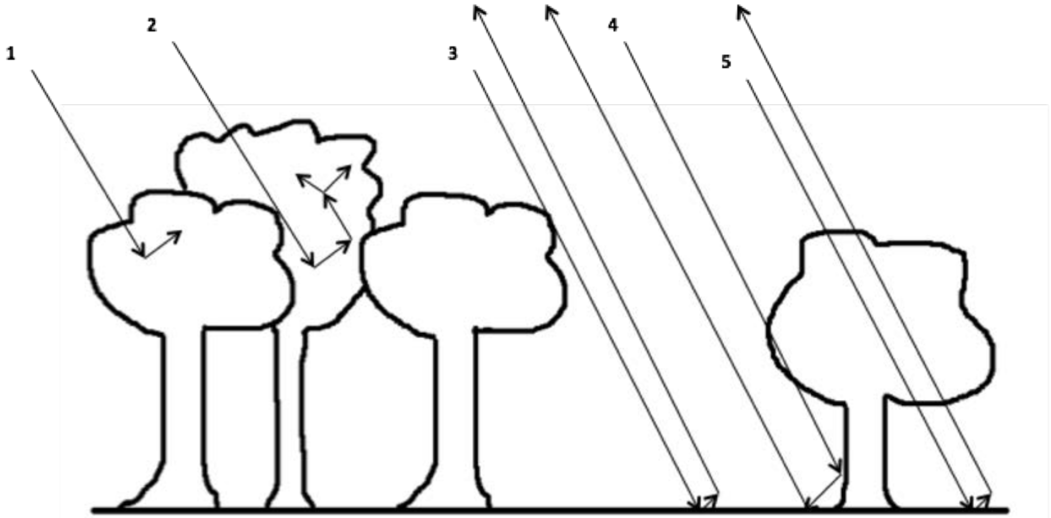

1: direct single scatter
2: multiple bounce
3: direct ground reflection
4: double bounce trunk - ground
5: attentuation of ground scatter by canopy

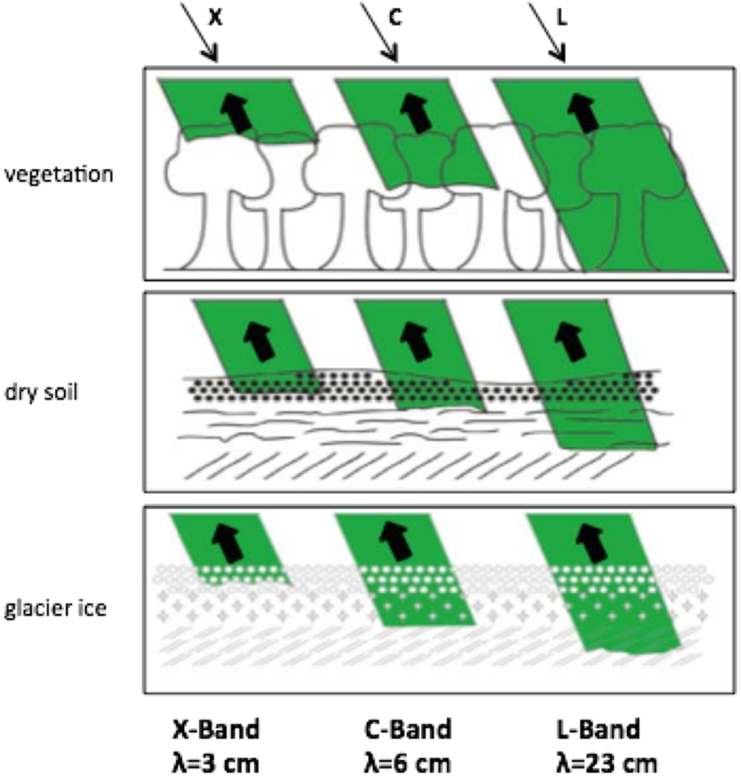

Image Tone - Example

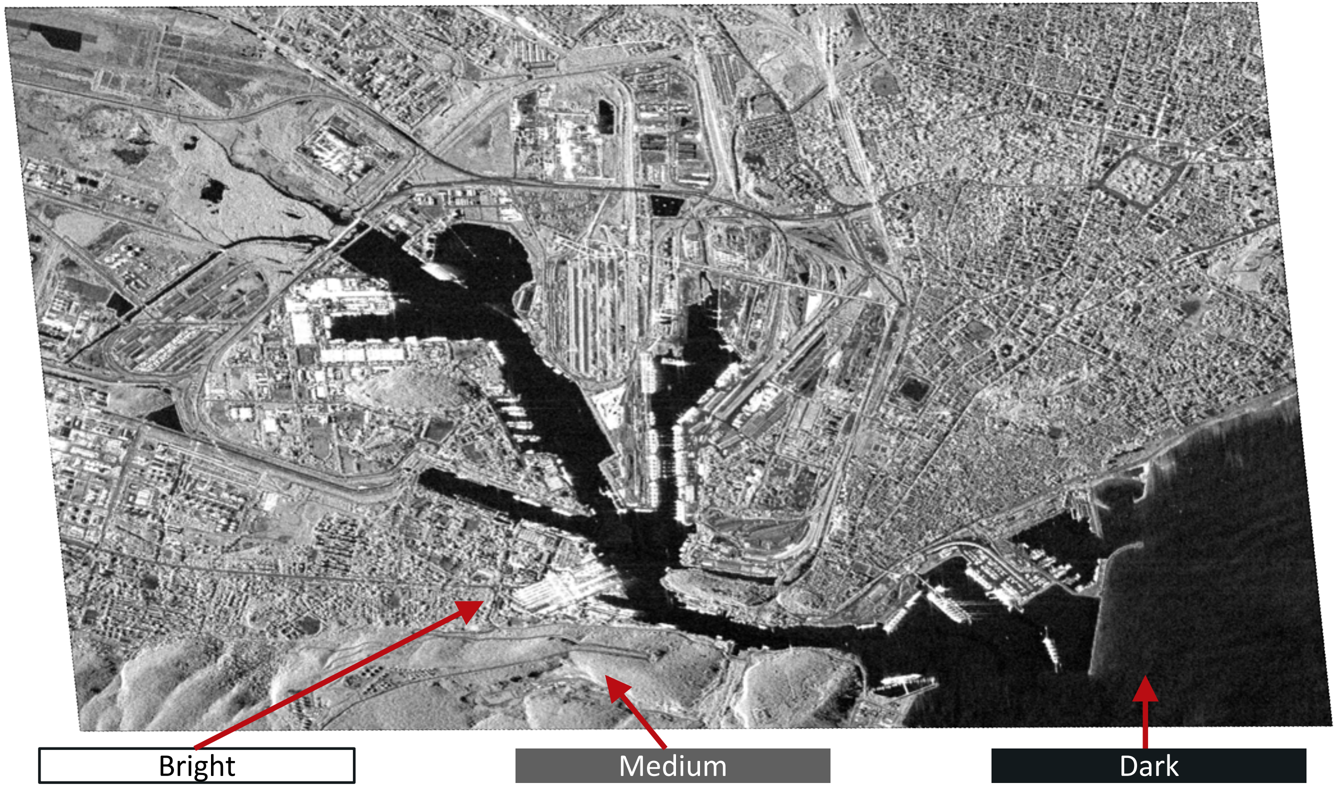

Port of Visakhapatnam, India © Astrium

Geometric Resolution

Geometric Resolution

- Size of the section of the Earth's surface that is encompassed by a single Pixel

Pixel

- = „Picture Element“
- Smallest entity of a digital image
- Raster grid cell with a well-defined gray value

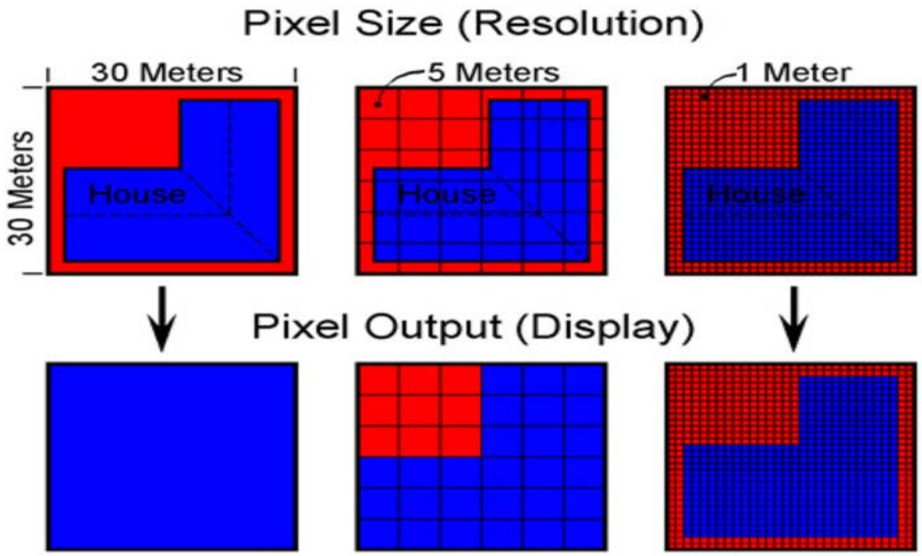

Radiometric Resolution

1-Bit	0 →	1
8-Bit	0 →	255
9-Bit	0 →	511
16-Bit	0 →	65.536
32-Bit	0 →	4.294.967.295

- Increasing Radiometric resolution = higher number of digital number values
- Higher resolution = finer gradation

← 1-Bit

16-Bit →

SAR Image Examples

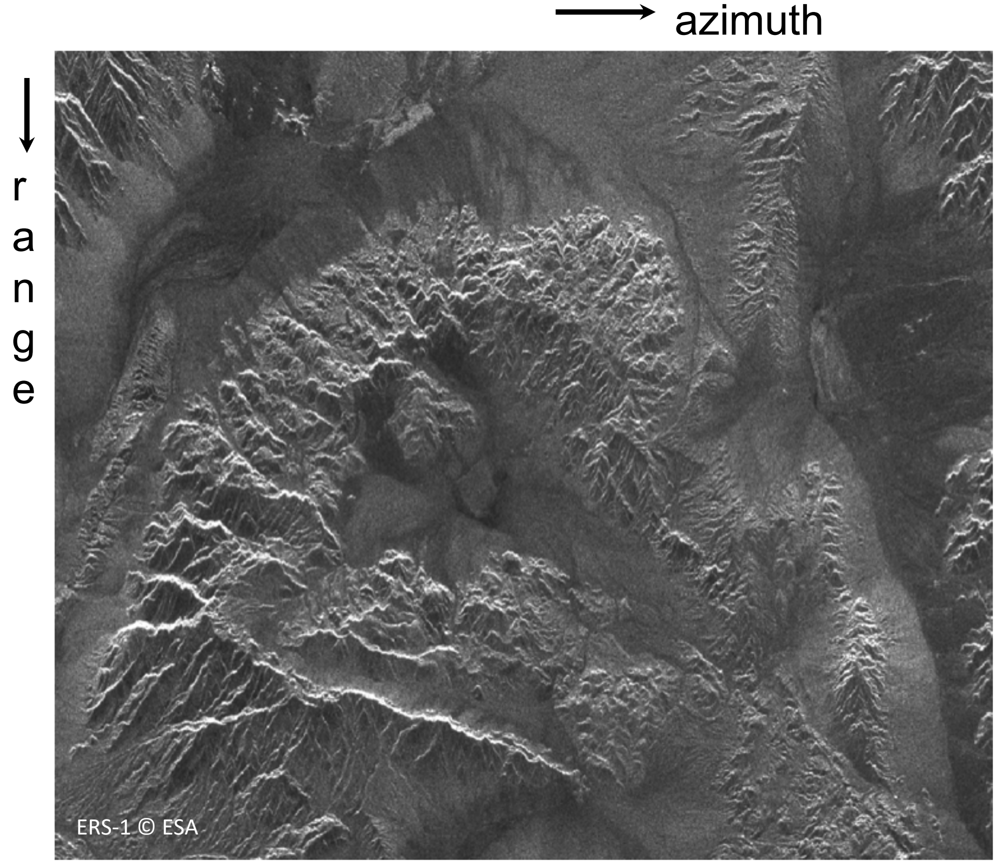

Sensor: ERS-1

Mojave Desert
CA, USA

Size ≈ 40 km x 40 km

Oil Signatures on Sea Surfaces

TerraSAR-X, July 9, 2010

Deepwater Horizon

Prestige Oil Tanker Disaster

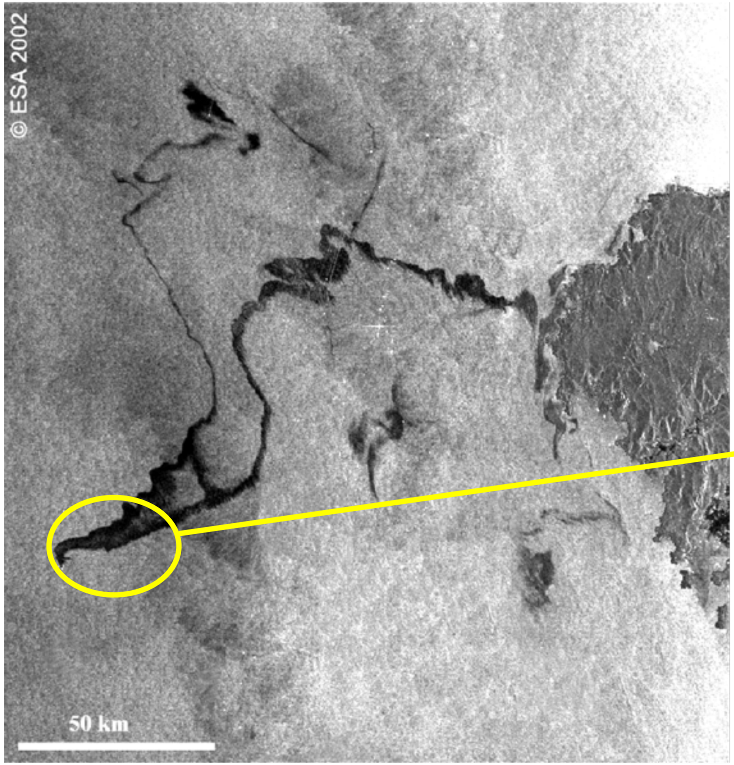

Envisat/ASAR
20 November 2002 © ESA

Heck der untergegangenen „Prestige", französisches Tiefsee-U-Boot „Nautile", Ölecks: *„Es ist leichter, auf dem Mond etwas zu reparieren*

KATASTROPHEN

Tschernobyl zur See

Sprengen mit Torpedos? Begraben unter Beton? Zuschweißen in 3800 Meter Tiefe? Experten rätseln, wie sie das Öl im Wrack der „Prestige" unschädlich machen können. Eine niederländische Firma will den Tanker auspumpen – es wäre die schwierigste Bergung der Seefahrtsgeschichte.

Es war nur irgendeine Konferenz, und kurz sollte sie auch sein. Deshalb hatte Geert Koffeman, Vizechef der weltweit operierenden Hochsee-Bergungsfirma Smit, kaum mehr als Aktentasche und Handy von Rotterdam mit nach London genommen. In der Firma daheim lief alles wie immer, Koffemans Leute zogen zwar gerade den Auftrag an Land, den manövrierunfähigen Tanker „Prestige" im Atlantik an den Haken zu nehmen – das aber klang für die Niederländer nach einem Routinejob.

Dann klingelte Koffemans Telefon, ein Kollege war dran: Die „Prestige" sei schwer beschädigt, vielleicht gar mache sie es nicht mehr lange. Koffeman griff sich schnellstens einen Einwegrasierer und eine Zahnbürste aus dem Notpack einer Fluggesellschaft und nahm die nächste Maschine nach Spanien.

Vor Ort begann Koffeman sofort, mit den zuständigen Behörden zu verhandeln: Er brauche einen Hafen, eine Bucht, wohin er die „Prestige" schleppen und wo er sie leer pumpen könne: Er ahnte, „das Schiff würde sonst auseinander brechen". Doch Francisco Alvarez-Cascos, Spaniens cholerischer Minister für Infrastruktur, lehnte ab. Teilnehmer eines Abendessens konnten ihn in sein Handy brüllen hören: Die Schlepper sollten das verdammte Ding gefälligst „al quinto pino" ziehen – „an den Arsch der Welt", egal, Hauptsache weit weg von Spanien.

Mit dem Befehl begann, was Spaniens Ministerpräsident José María Aznar jetzt reumütig als „die größte Umweltkatastrophe unserer Geschichte" bezeichnet – und was dem Bergungsprofi Koffeman bald schon einen der schwierigsten Aufträge in der Geschichte der Seefahrt einbringen könnte. Denn wo die „Prestige" vor vier Wochen auseinander brach und sank, ist der Atlantik 3800 Meter tief, das Wrack damit unerreichbar für normales Bergungsgerät. Knapp 20 000 Tonnen Schweröl hat das Schiff bislang verloren, nahezu 60 000 Tonnen sind noch an Bord, jeden Tag sickern 125 davon in den Ozean.

An die tausend Kilometer der spanischen Küste sind zumindest teilweise verseucht. Bald kann das Öl auch Frankreichs Traumstrände zwischen den Pyrenäen und Biarritz erreichen – nie zuvor waren die Auswirkungen einer Tanker-Katastrophe verheerender.

Tiefes Grab

Lage bekannter Wracks nach Meerestiefe in Metern

156

DER SPIEGEL 51/2002

Der Spiegel, 51/2002

Creating colour with RGB composites

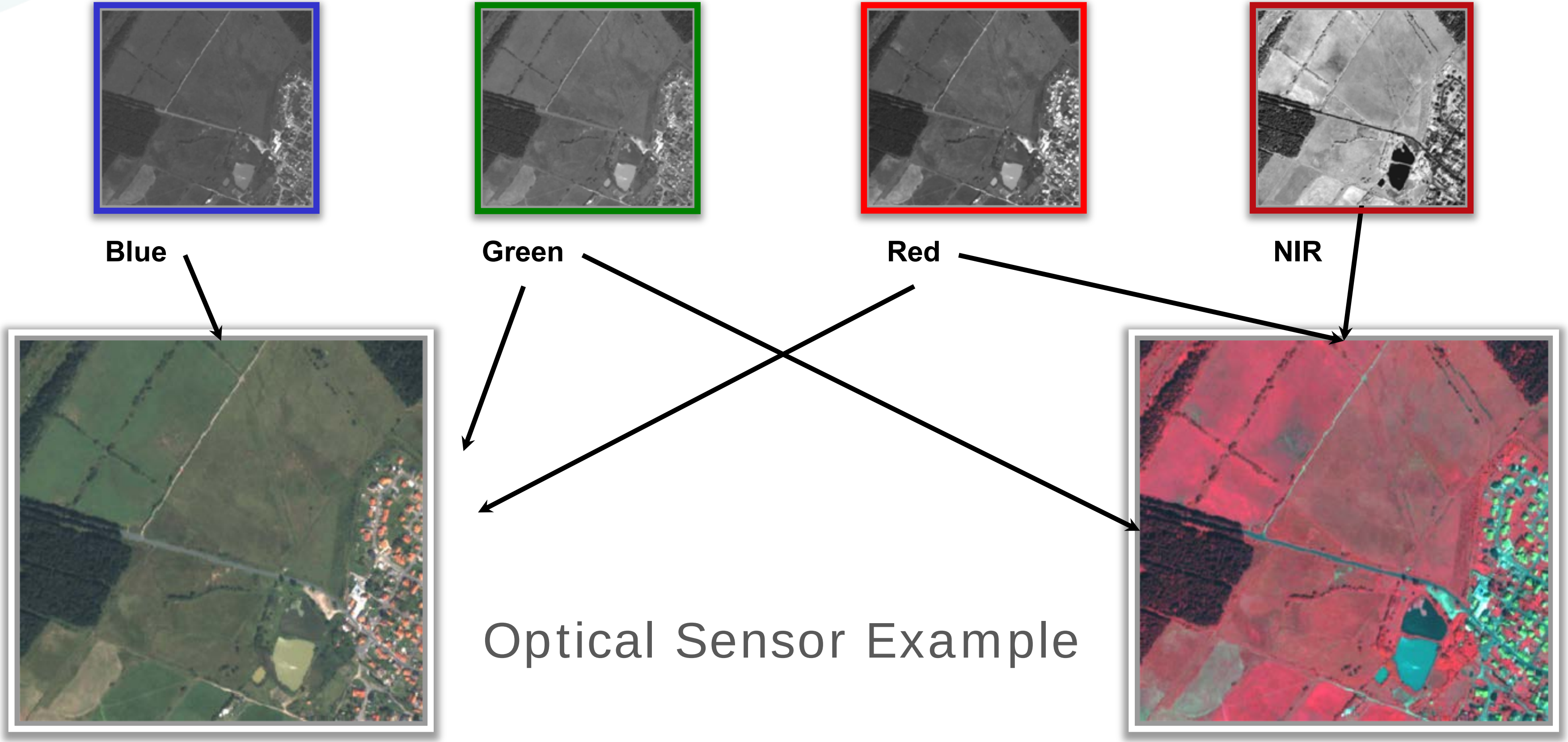

Multi-Temporal composites

- Combination multiple dates of SAR acquisitions
- Colors indicating changes

© Google Earth

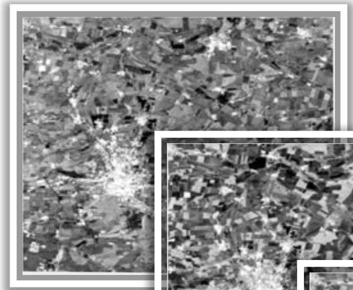

TSX (HH)
06APR12

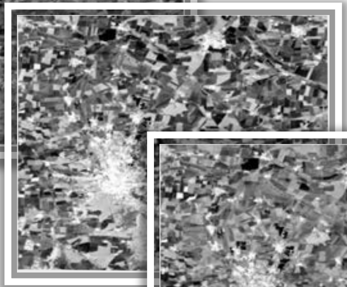

TSX (HH)
20MAY12

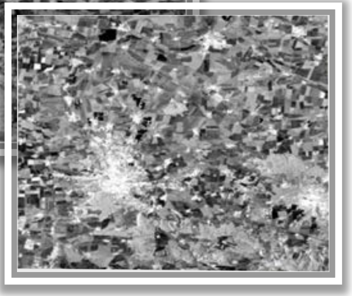

TSX (HH)
31MAY12

R: 06APR | G: 20MAY | B: 31MAY

Multi-Frequency composites

- Combination of multiple SAR frequency bands
- Synergy of different backscatter mechanisms

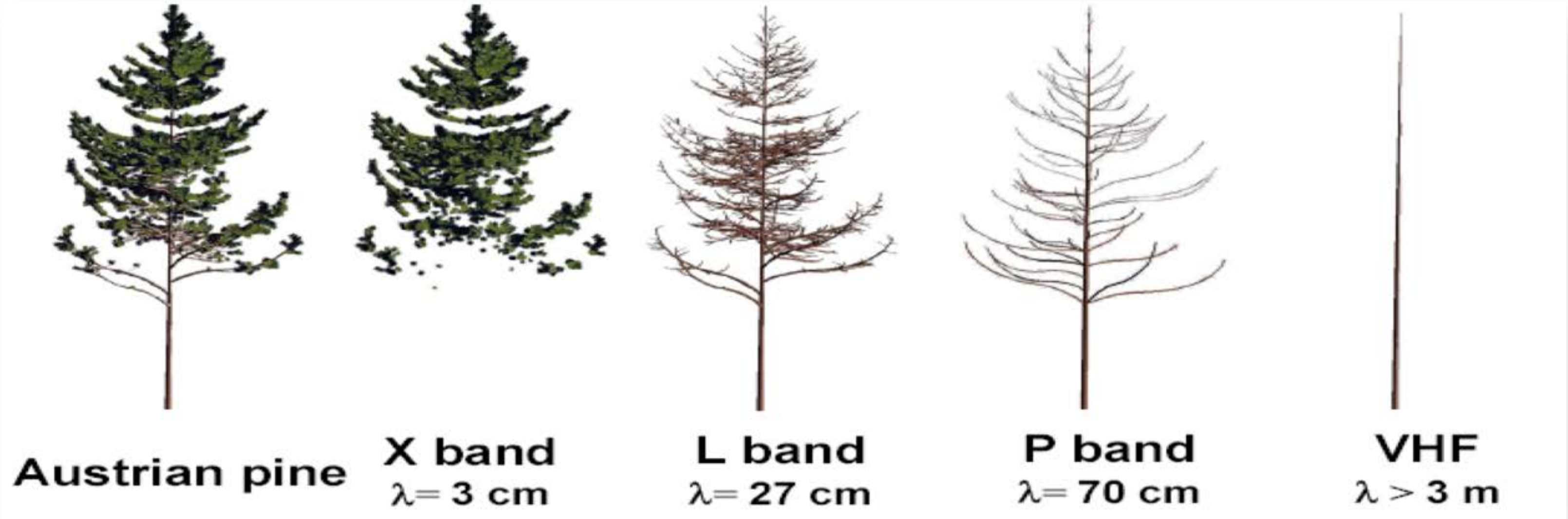

Multi-Frequency composites

- Combination of multiple SAR frequency bands
- Synergy of different backscatter mechanisms

Landsat R: B 1 G: B 2 B: B 3

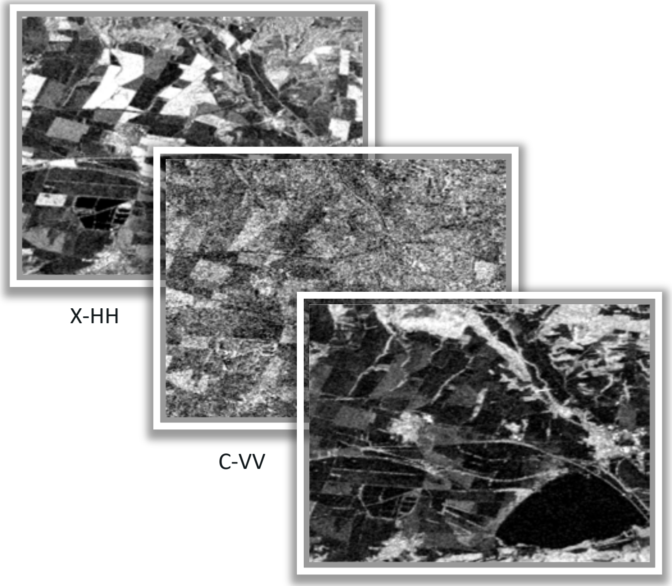

X-HH

C-VV

L-HH

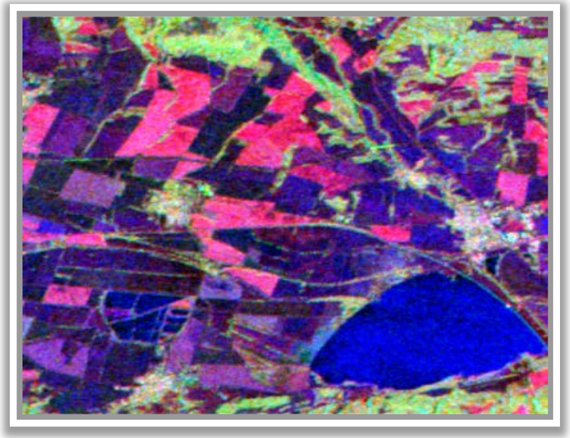

R: X-HH | G: L-HH | B: C-VV

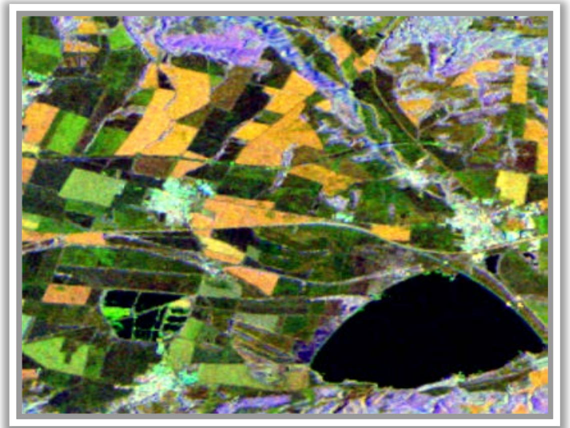

R: X-HH | G: L-HH | B: X-HV

Multi-Polarisation Products

- Combination of multiple polarisations
- Colours indication different backscatter mechanisms

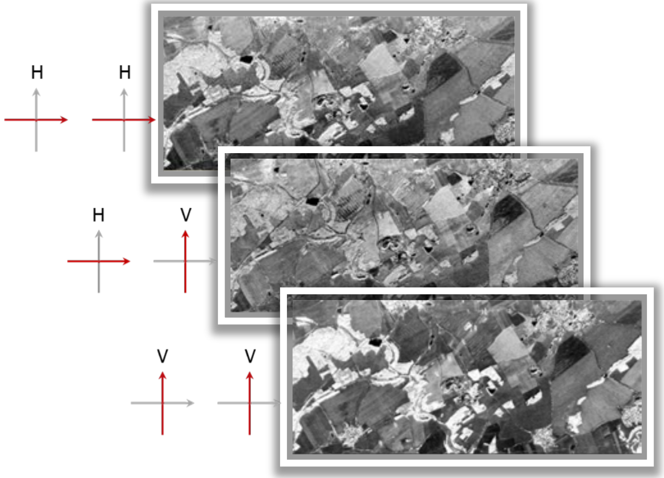

R: HH | **G:** VV | **B:** HV

Multi-product composites

- Combination of multiple products
- Increased class separability

© Google Earth

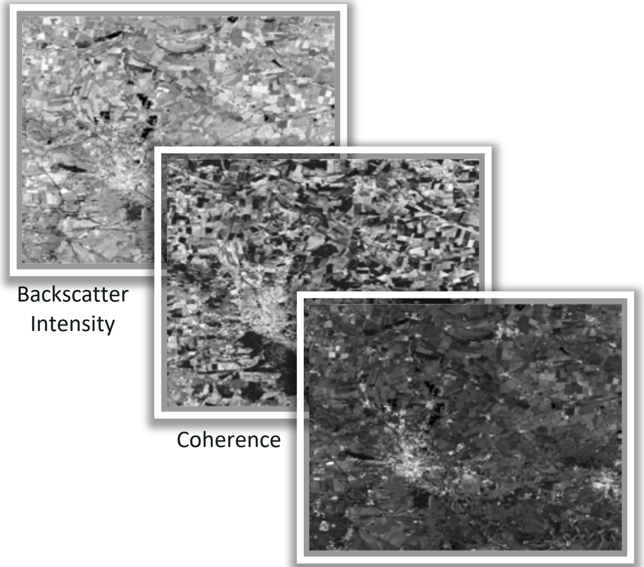

Backscatter Intensity

Coherence

Average Backscatter

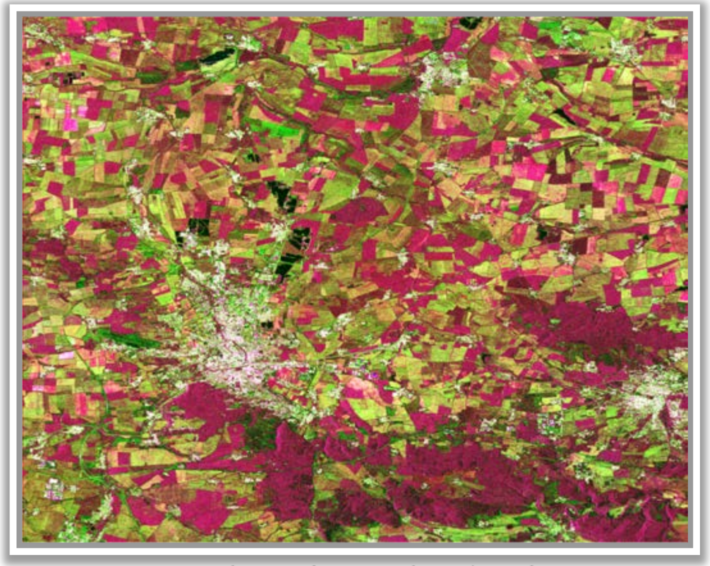

R: Intensity | G: Coherence | B: Ø Backscatter

SAR and snow/ice

The SAR backscatter from snow and ice surfaces is dependent from various variables including:

- Liquid water content
- Grain size & layering
- Density
- Salinity
- Surface roughness
- Wavelength
- Polarization
- Incident angle
- .....

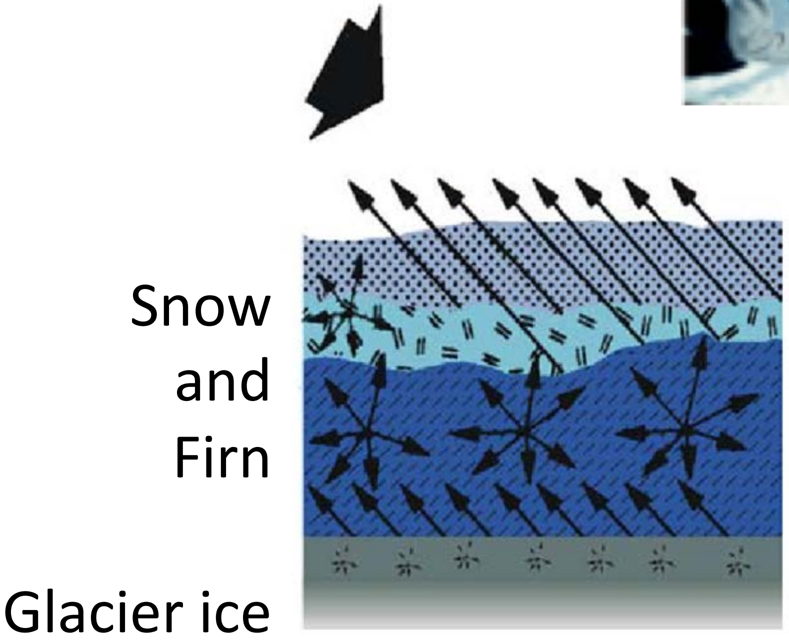

Rau, 2004

Absorption and penetration depth

$$\varepsilon = \varepsilon' - i\varepsilon''$$

ε': Real part of the dielectric constant ➔ Reflection
ε'': Imaginary part of the dielectric constant ➔ absorption

The real part of the dielectric constant of ice is almost constant throughout the microwave region (value of 3.17). The real part of the dielectric constant of dry snow only dependend on snow density. Rees (2006) gives the following expression:

$$\varepsilon' = 1 + 1.9\,\rho_s$$

with ρ_s in Mg/m^{-3}

➚ Penetration depth (δ_p):

$$\delta_p = \frac{1}{\kappa_e} = \frac{1}{(\frac{2\pi}{\lambda_0})(\frac{\varepsilon''}{\varepsilon'^{0.5}})}$$ für ε''/ ε'' << 1

Absorption and penetration depth

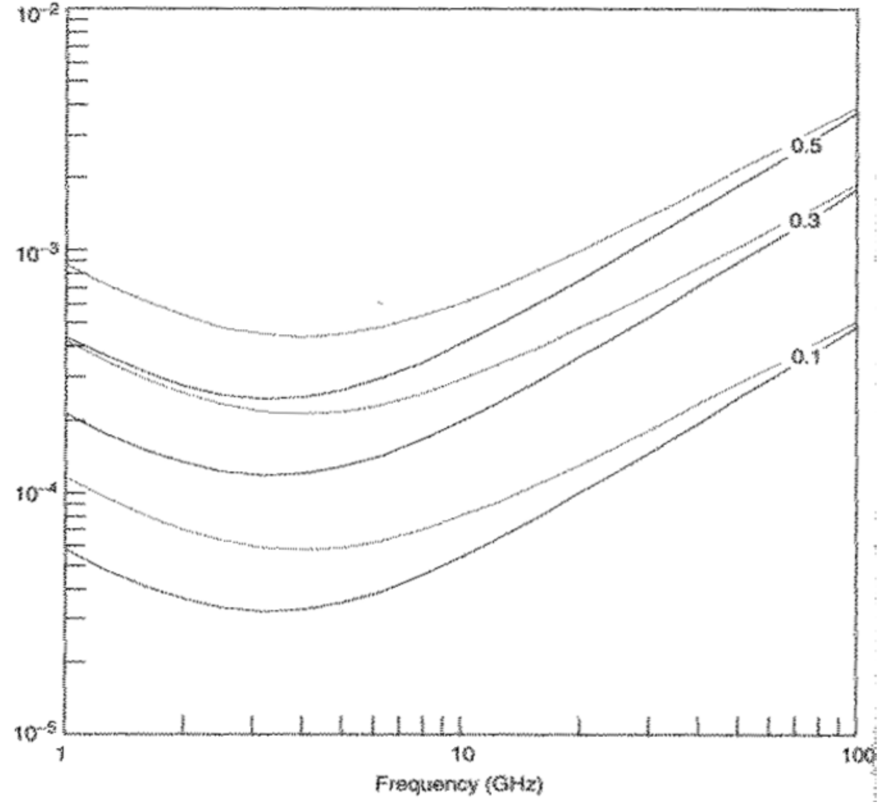

Imaginary part of the dielectric constant of dry snow.
Curves for Mgm^{-3} density of snow

Rees, 2006
(after Mätzler & Wegmüller, 1987; Tinga et al., 1973)

Absorption and penetration depth

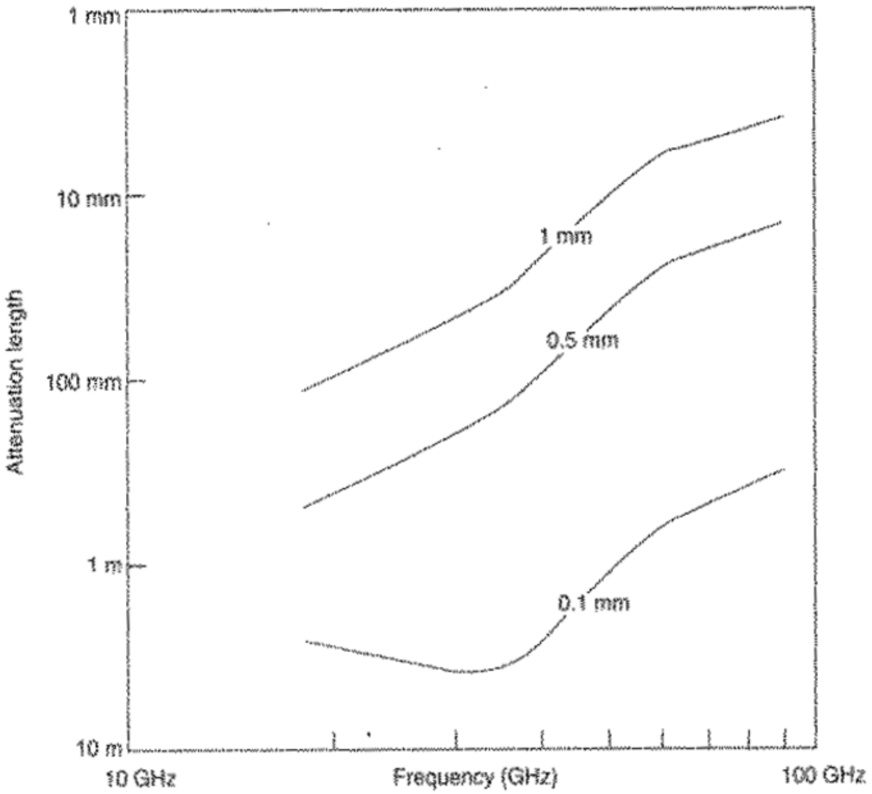

Empirical attenuation lengths in snow as a function of grain radius and frequency

Rees, 2006 (after Hallikainen et al., 1987)

Absorption and penetration depth

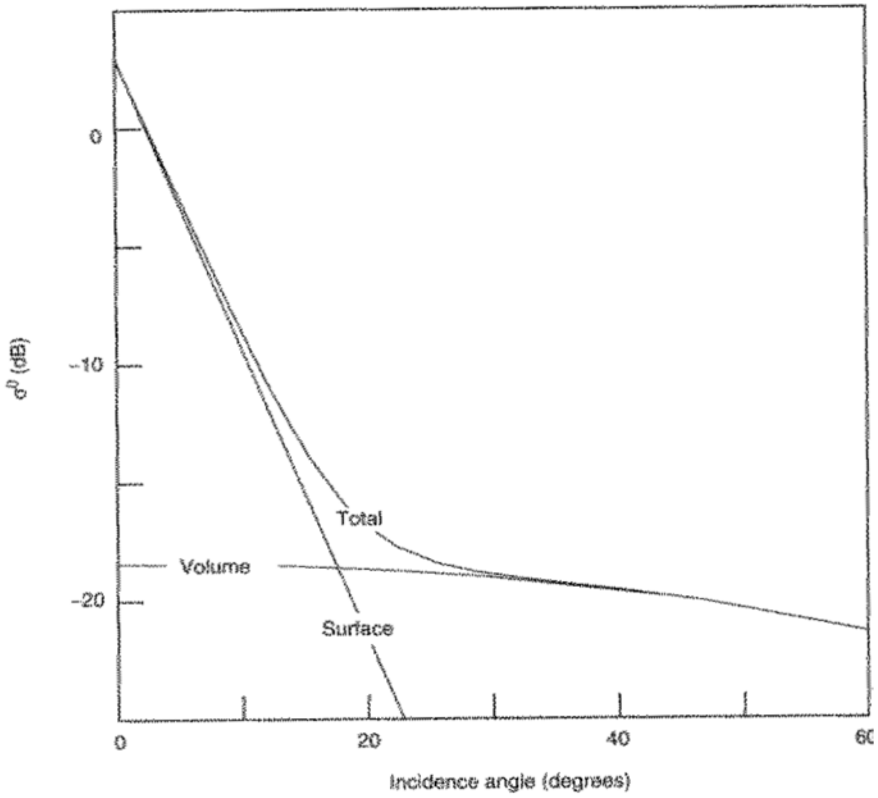

Typical variation of co-polarized backscattering coefficient with incident angle for wet snow

Rees, 2006 (after Hallikainen et al., 1987)

Surface roughness

- Generally described as height difference to a reference surface / length expressed as mean height, standard deviation of autocorrelation length

- As a rule of thumb a surface can be regarded as smooth (specular reflection) when the height difference is smaller as the wavelength
  - In case of the roughness of the surface equals $n*\lambda/2$, Bragg resonance is observed
  - In case of the mean roughness of the surface in the same magnitude as the wavelength, diffuse reflection occurs

Surface roughness

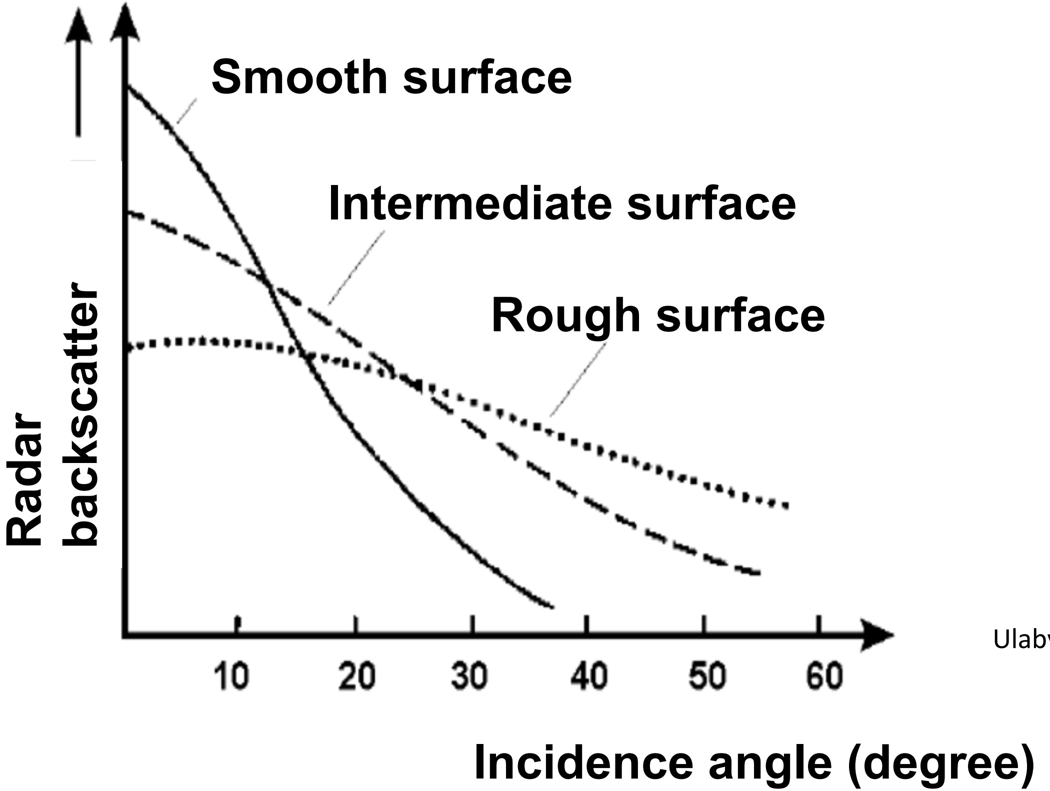

Ulaby et al. 1986

Backscatter coefficients

Backscatter coefficients at different incident angles (VV, 5.3 GHz), snow

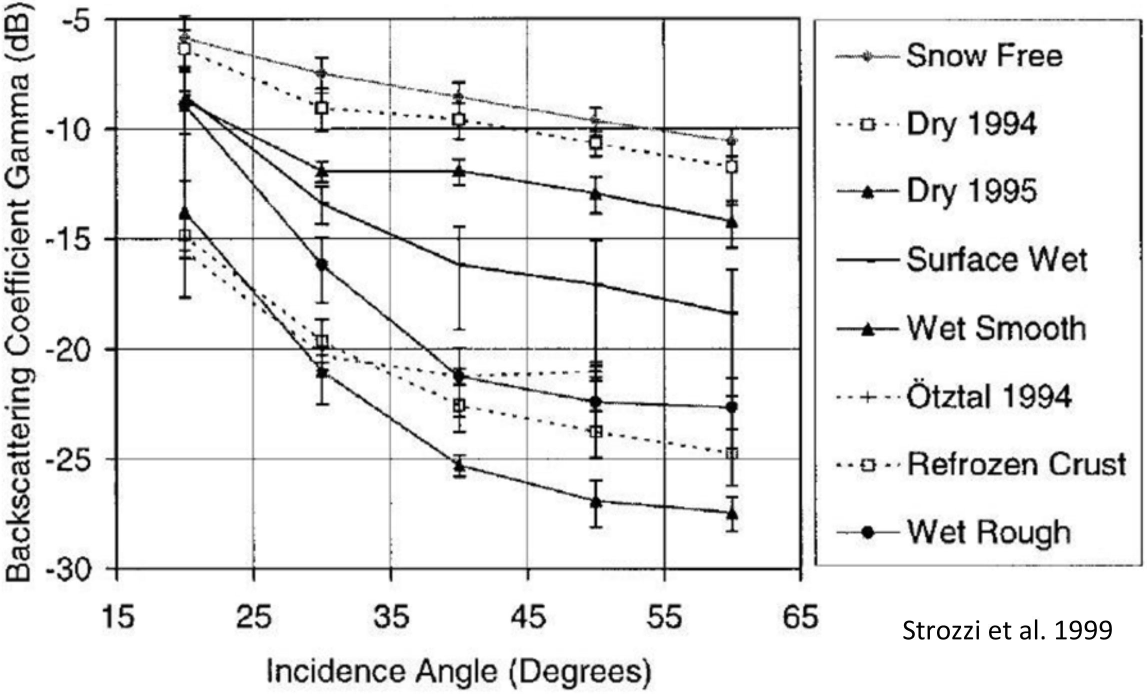

Strozzi et al. 1999

Implications

- Snowpack structure influences backscatter signal
- Sensor viewing geometry influences backscatter strength
- Surface conditions of the snowpack considerably influence the SAR backscatter signal strength
- Liquid water content of the snowpack minimizes the penetration depth of the SAR signal
- Changes in surface conditions can influence location of the scattering centers in repeat acquisitions and hence impact interferometric analysis

Radar glacier zones

- Snow and radar glacier zones from C-band, VV SAR and glaciological facies zones

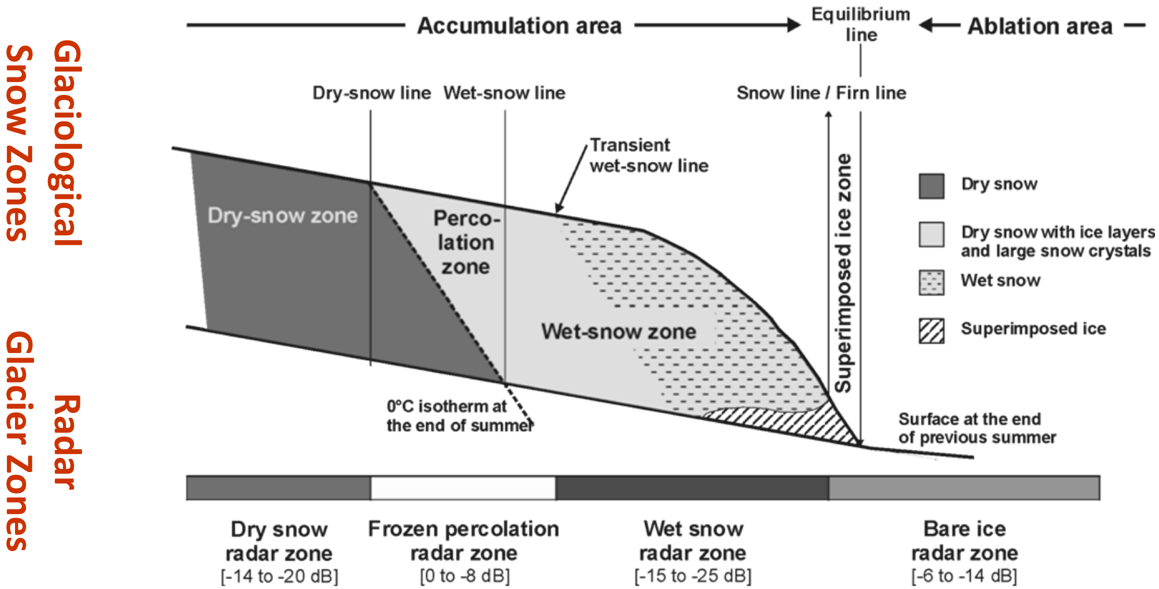

Rau et al., 2000, modified after Paterson, 1994

Radar glacier zones

- <u>Dry snow zone (DSZ):</u>

Absence of any surface melt, consequently small snow grain size (interior of the large ice sheets, high elevations)

- Little volume scattering and thus low backscatter with no significant seasonal variation

- Spatial variability of backscatter related to grain size variations

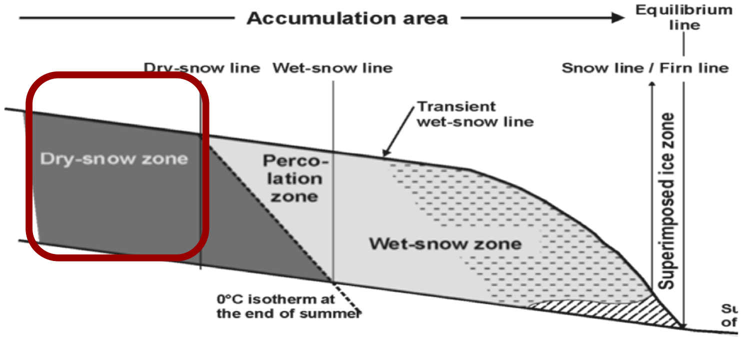

Radar glacier zones

- <u>(Frozen) percolation zone:</u>

wet snow metamorphism occurs with formation of ice lenses and large snow grains

- Very high backscatter from volume scattering during frozen conditions

- Low backscatter when wet

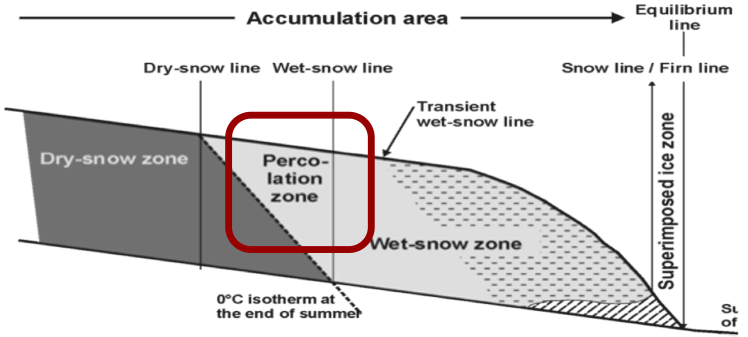

Radar glacier zones

- <u>Wet snow zone:</u>

melt conditions, liquid water present, absorption,

- Low backscatter with penetration depth reduced to upper centimetres of the snow cover

- Surface roughness can cause high backscatter
  e.g. from sun cups

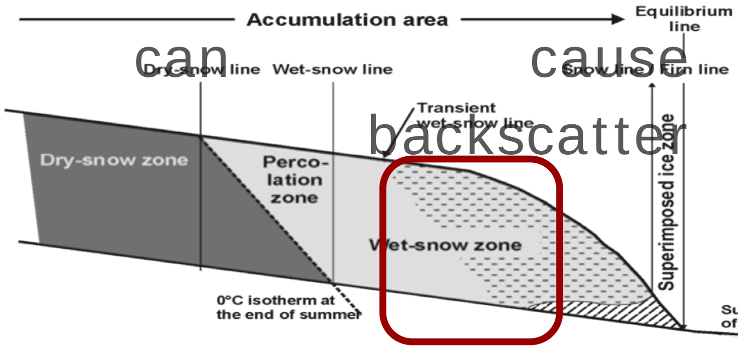

Antarctic Peninsula

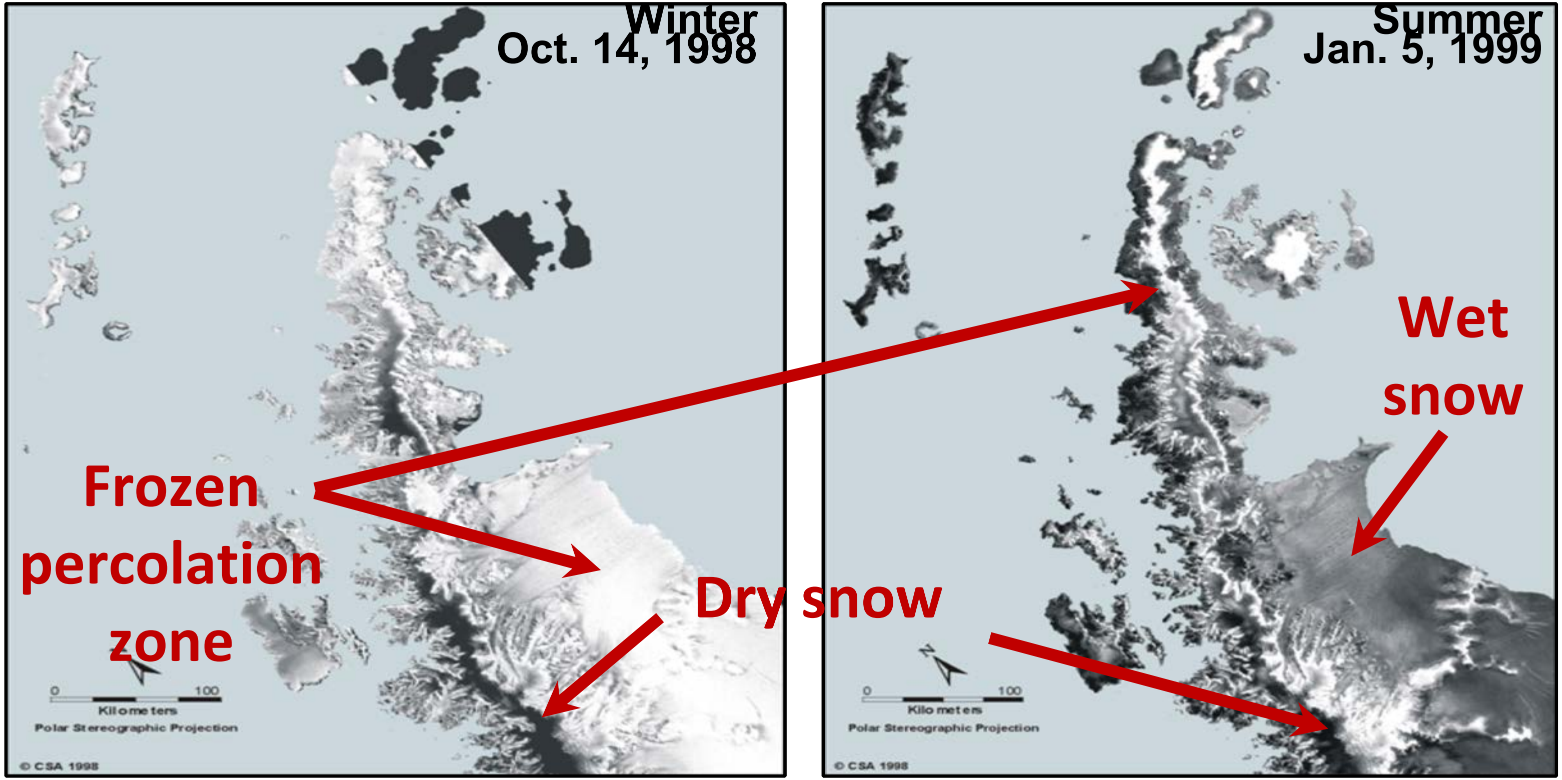

Fig. 8: Rau, 2004

Radar glacier zones

- Bare glacier ice: specular reflector at the ice surface

- Lower backscatter than the frozen wet/percolation-snow zone in winter
- During melt
backscatter of
zone appears
wet-snow zone

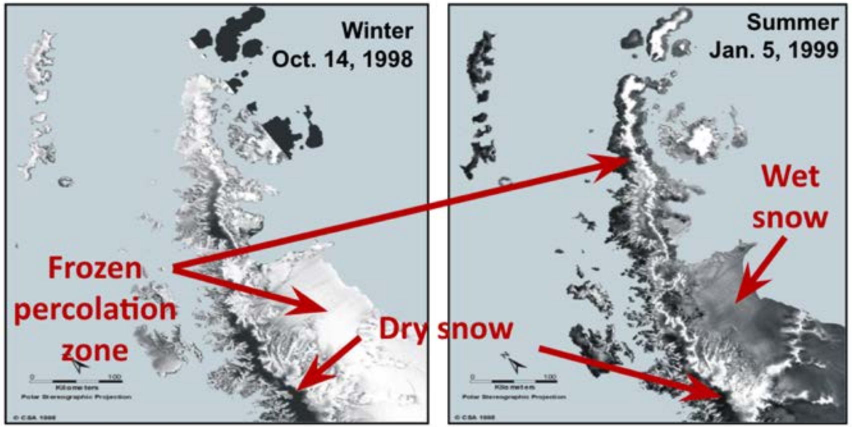

Radar glacier zones

- The boundary between the bare-ice facies and the wet-snow facies is distinct, which allows the determination of the <u>snow line</u>

- <u>Non-glacierized areas:</u> on single SAR images often difficult to separate from bare glacier ice due to similar backscatter. However, multi-temporal coverage support clear separation as well as coherence (e.g. ice towards rocky surface in the surroundings of glaciers)

Seasonal SAR backscatter

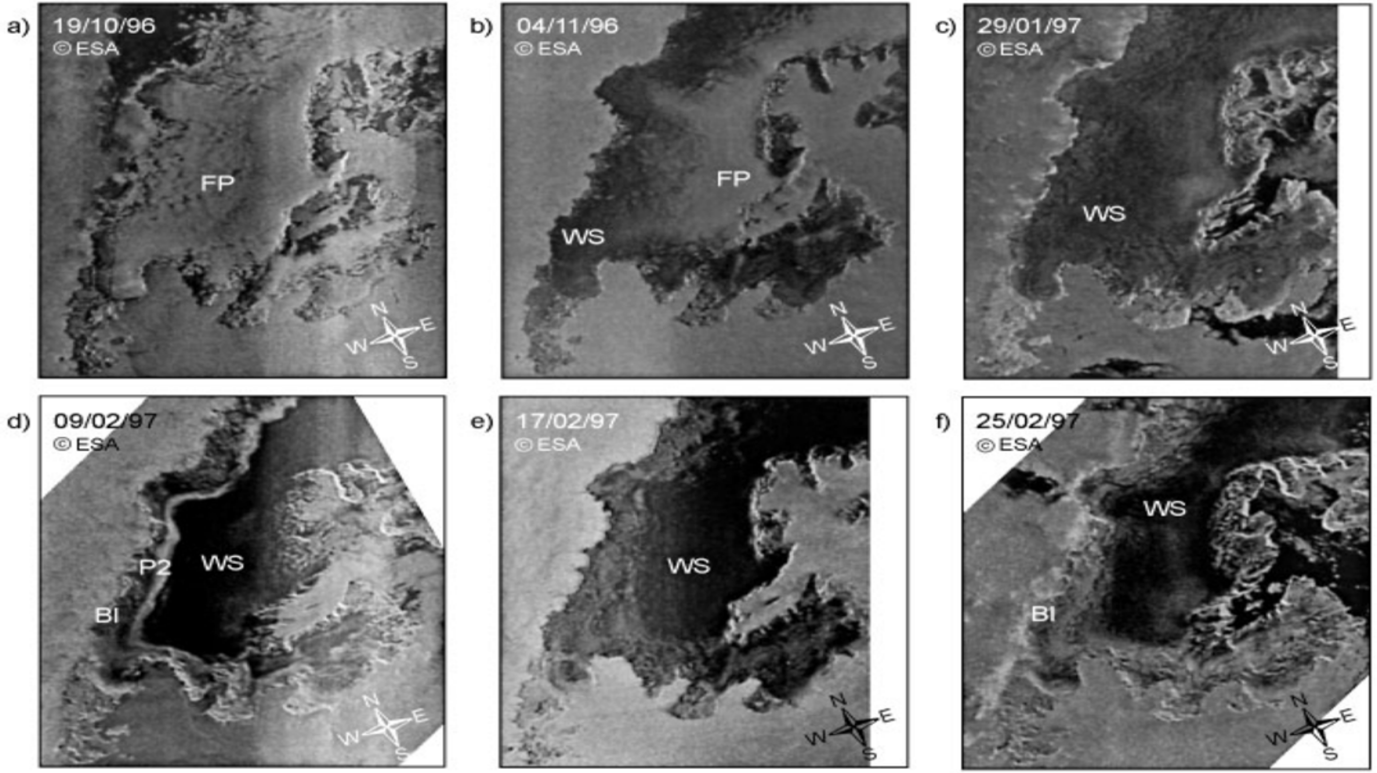

King George Island, Antarctica
C-band, VV

WS: wet snow
FP: frozen percolation
BI: bare ice
P2: rough wet snow

Braun et al., 2000

Seasonal backscatter

Seasonal development
of ERS backscatter
King George Island
Antarctica

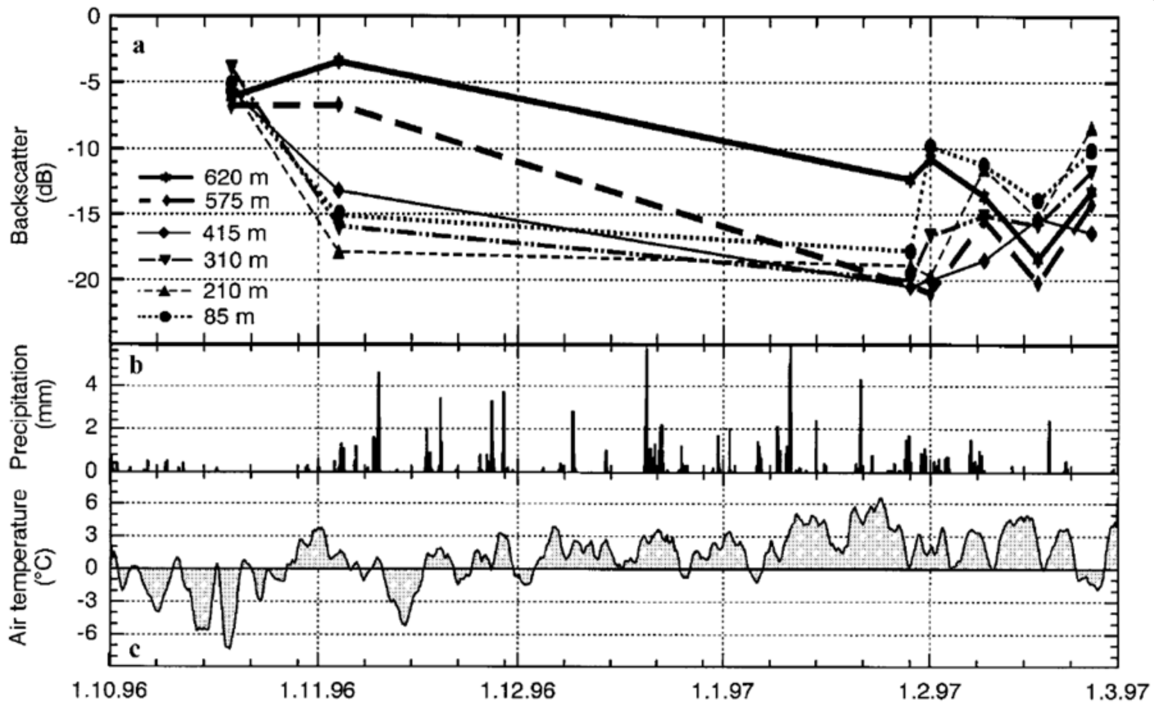

Braun et al., 2000

Multi-temporal Color Composite

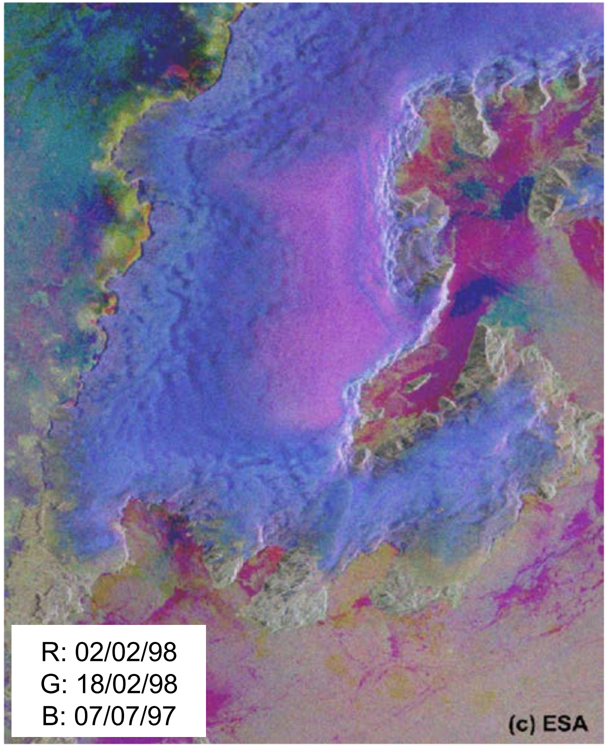

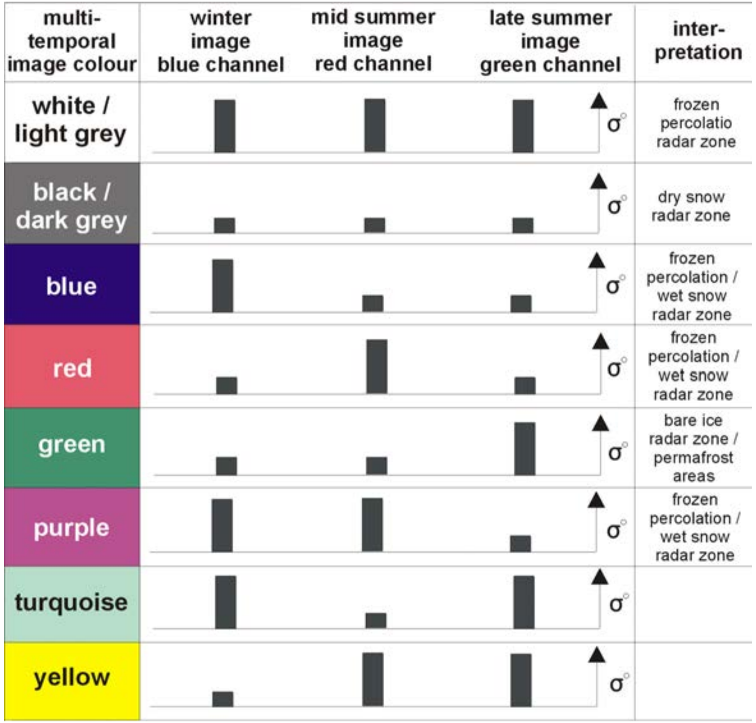

Braun et al., 2000

Influence of polarization and frequency

Austre Okstindbreen (Svalbard)

- HV show more variation in backscatter
- better separation of firn line with cross-polarization

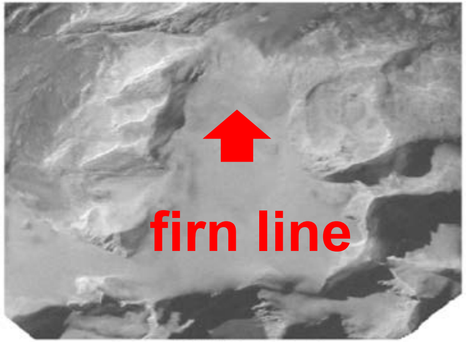

C-Band HH-Polarisation

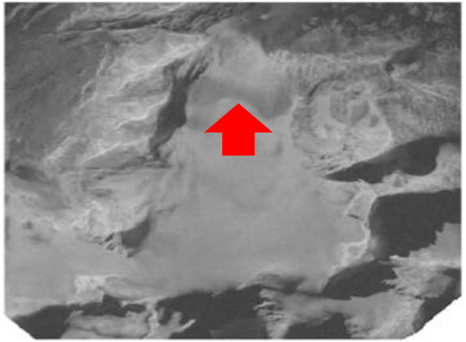
C-Band HV-Polarisation

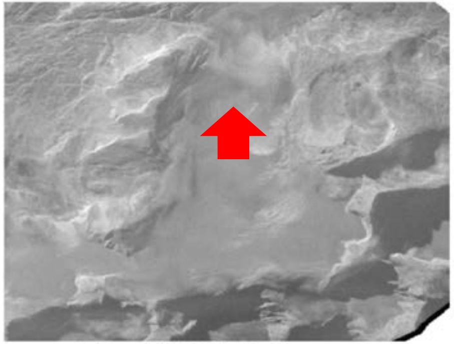
L-Band HH-Polarisation

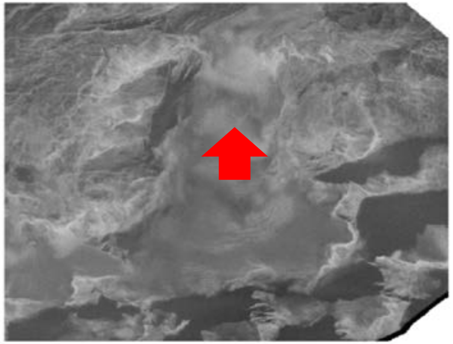
L-Band HV-Polarisation

König et al., 2000

Influence of polarization and frequency

Austre Okstindbreen (Svalbard)

- Center line profile

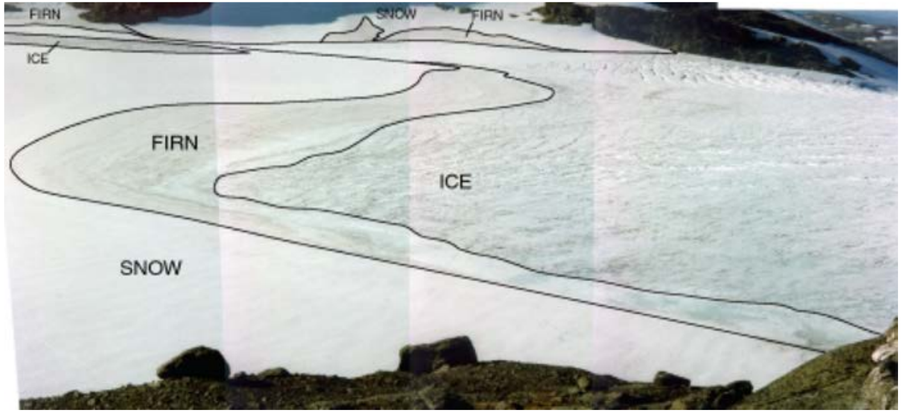

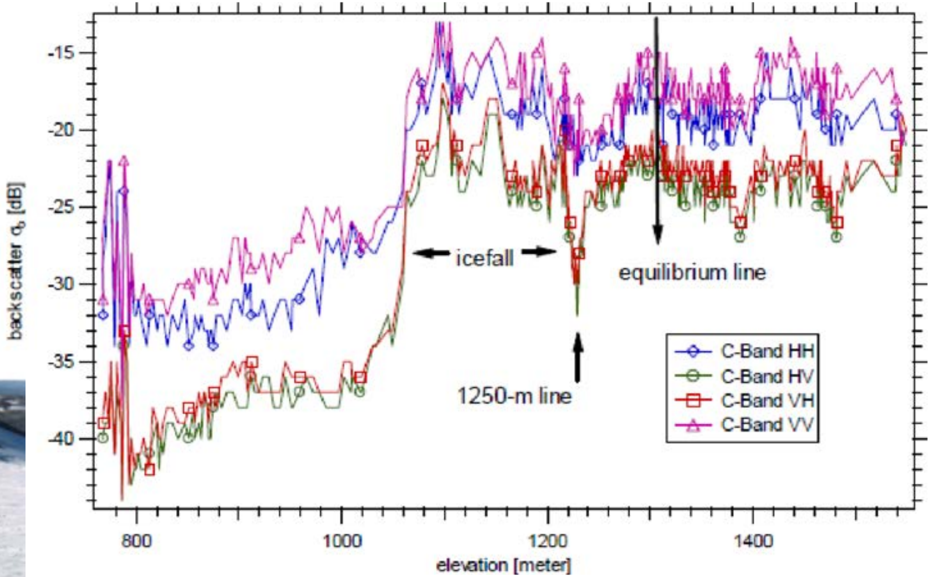

König et al., 2000

Hands-on Exercise

- Introduction on how to discover, access and process EO data
- Simple snow and ice classification, glacier velocity and multi-temporal composites
- Using Jupyter Notebooks, ESA SNAP Toolbox and OpenSearch Catalogues

Data Challenges

- Identify Data Challenges where Earth Observation products can provide a solution
- Provide community open science tool, where EO satellite data and derived products can be accessed, visualised, processed, shared and validated.
- Joint-H2020 opportunity to network and propose the development of EO-based applications and research

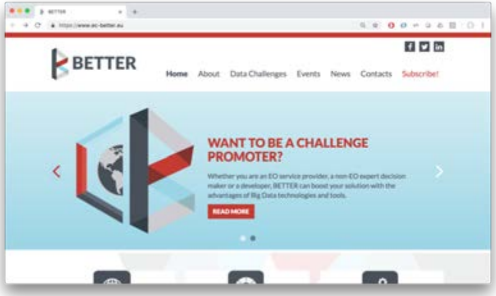

Ice Classification

- Proponent
  - Sascha Schiøtt (sasc@natur.gl)
  - Greenland Institutet of Natural Resources

- Ilulissat Icefjord - N69 7 60 W49 30 0
  - *We want to see if there has been some changes in the last 4 years to the average ice cover distribution and (or different types of ice) in the northern and southern branch of the fjord system*
  - *And also the position of the glacier front at the central branch of the fjord system.*

Sea Ice Concentration

- Proponent
  - Takuya Nakanowatari (nakanowatari.takuya@nipr.ac.jp)
  - Arctic Environment Research Center
    National Institute of Polar Research
- Northern Sea Route
  - Region: 100E-180W, 70-80N
  - *Since I would like to make the SIC data covered this ship trajectory, please give the recommended method and/or provide the tool to make the SAR product as demonstrated in the afternoon (it seems to be difficult for me)*

Natural Oil Seeps Detection

- Proponent
    - Leendert Vergeynst (leendert.vergeynst@bios.au.dk)
    - Arctic Research Centre, Aarhus University, Denmark
- Vaigat, Disko Bay
    - To detect oil sheen on the water surface in the offshore area near the known oil seeps based on historic satellite data. Such data could help us to identify locations of interest for sampling during the cruise.

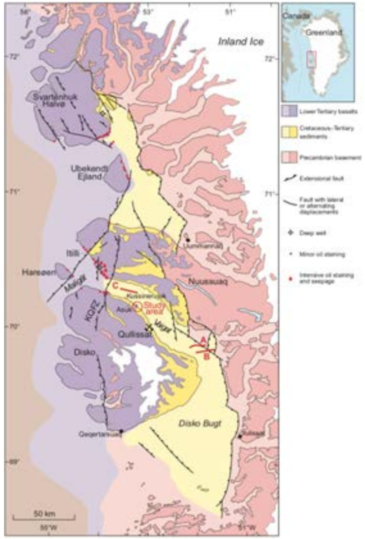

Temporal Series of Backscatter

- Proponent
  - Agata Grynczel (grynczel@iopan.gda.pl)
  - Institute of Oceanology of the Polish Academy of Sciences
- North of Fram Strait

  the passage between Greenland and Svalbard
  located roughly between 77°N and 81°N

- Temporal Series of Backscatter for 2016

Land-fast ice extenrt

- Proponent:
  - Joshua Jones
  - University of Alaska Fairbanks
- Alaskan Arctic, around Barrow and Wainwright
  - December through July 2018
- Objective is to compare the land-fast ice extent visible in the satellite imagery to the observations made in these communities

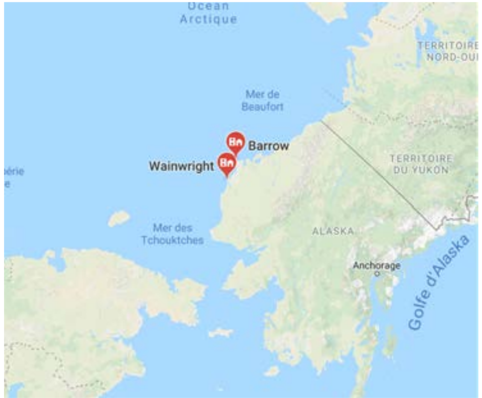

TERRADUE

Looking forward hearing from you!

https://www.terradue.com

Pedro Gonçalves
pedro@terradue.com